Selective and Chemical-Free Removal of Toxic Heavy Metal Cations from Water Using Shock Ion Extraction

Mohammad A. Alkhadra, Matthew L. Jordan, Huanhuan Tian, Christopher G. Arges, and Martin Z. Bazant*

Cite This: *Environ. Sci. Technol.* 2022, 56, 14091−14098

Read Online

ACCESS | Metrics & More | Article Recommendations | Supporting Information

ABSTRACT: Electrochemical methods are known to have attractive features and capabilities when used for ion separations and water purification. In this study, we developed a new process called shock ion extraction (shock IX) for selective and chemical-free removal of toxic heavy metals from water. Shock IX is a hybrid process that combines shock electrodialysis (shock ED) and ion exchange using an ion exchange resin wafer (IERW), and this method can be thought of functionally as an electrochemically assisted variation of traditional ion exchange. In particular, shock IX exhibits greater ion removal and selectivity for longer periods of time, compared to the use of ion exchange alone. The use of an IERW in shock ED also increases multivalent ion selectivity, reduces energy consumption, and improves the hydrodynamics and scalability of the system.

KEYWORDS: water purification, selective separations, electrokinetics, ion exchange, heavy metals
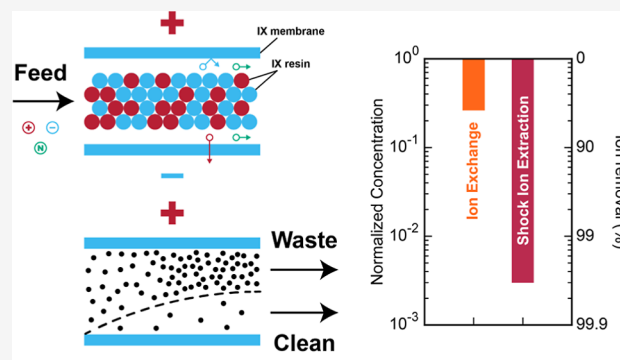
1. INTRODUCTION

Toxic heavy metal contaminants in water represent a significant hazard to human and animal health and to environmental safety. Heavy metal pollution and its concomitant challenges are exacerbated by the large number of candidate pollutants, many of which are extremely toxic and difficult to selectively remove from water. These species contaminate water by various means, such as erosion or leaching of natural deposits (e.g., cadmium, selenium, and radium), corrosion of plumbing materials (e.g., copper, zinc, and nickel), and discharge from refineries and heavy industries (e.g., chromium, arsenic, mercury, cobalt, and antimony). Common methods for removal of heavy metals—often present in trace quantities—from water include adsorption,[1,2] coagulation,[3,4] filtration,[5−7] and ion exchange,[8−12] though these systems are costly and require either regular chemical regeneration or frequent replacement of materials.[1,4,13] In this article, we adapt an emerging chemical-free method for electrokinetic deionization known as shock electrodialysis (or shock ED)[14−17] and for the first time incorporate ion exchange resin wafers (IERWs)—a recent innovation[18−20] in the materials science of ion exchange—to selectively remove heavy metal cations from contaminated water. We call this new method "shock ion extraction" (shock IX) since it is a hybrid process that combines shock ED and ion exchange. We demonstrated in previous experimental[16,17,21] and theoretical[22,23] work that shock ED is intrinsically selective toward multivalent ions, and we show here that the use of an IERW—

composed of a strong acid cation exchange resin and strong base anion exchange resin—further increases this selectivity. Moreover, the use of an IERW reduces energy consumption and improves the hydrodynamics of the system by providing regions of high fluidic permeability in a hierarchical pore structure. Shock IX is similar in certain ways to the established method of electrodeionization (EDI),[24] which is a continuous process used to deionize and polish feeds that are typically dilute to begin with. Unlike shock IX, however, EDI displays limited multivalent selectivity, despite the presence of selective ion exchange resins,[25−27] which makes it more appropriate when the goal is to remove all dissolved species.

Separation of multivalent ions by shock ED, irrespective of the kind of porous material used, relies on the action of a deionization shock wave,[28] which produces a sharp concentration gradient near an ion selective surface such as a cation exchange membrane[14,29] or a metal electrodeposits.[30,31] This shock wave is generated when overlimiting current is applied (i.e., when transport of ions is faster than by diffusion alone), and it is sustained in the system due to the presence of a charged porous material.[29,32,33] While overlimiting current in
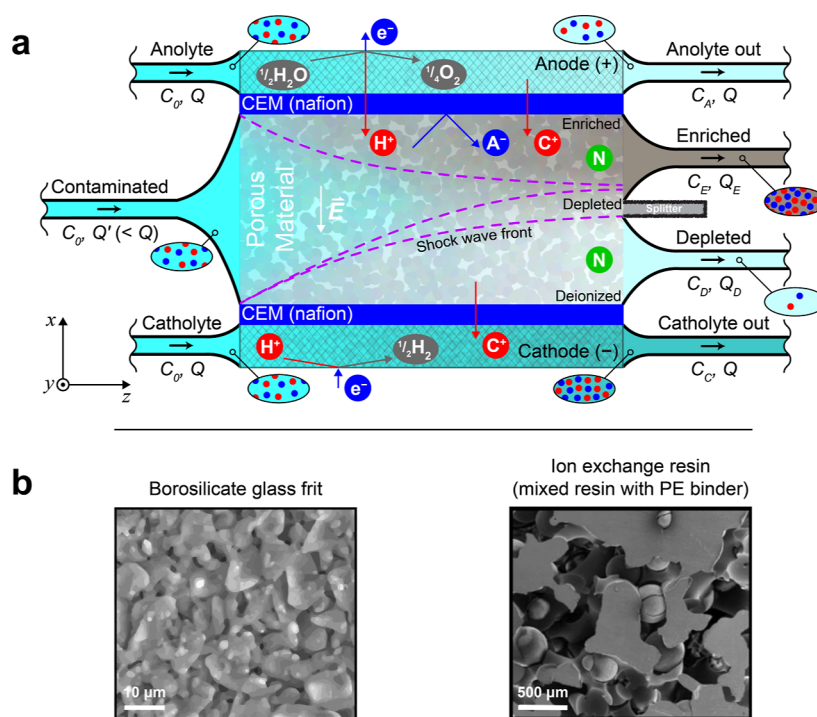
Figure 1. Schematic of the governing principles of shock ED and shock IX. (a) Rectangular cross section of the device shows water splitting at the anode and formation of molecular hydrogen at the cathode (maintained under acidic conditions to prevent precipitation of metal hydroxides), which are the primary electrochemical reactions that provide current to the cell. Contaminated water in the porous material is then subjected to an electric field ($\bar{E}$) that transports charged species (labeled as C$^+$ for cations and A$^-$ for anions) perpendicular to the flow. Anions are blocked by cation exchange membranes, and neutral species (labeled N) are unaffected by the electric field. For each stream, the flow rate is denoted by the letter Q and concentration by the letter C; streams are colored based on the relative concentration of ions. (b) Scanning electron microscopy images of the two porous materials used in this study, one of which is a borosilicate glass frit (shock ED) and the other is an IERW (shock IX). Image of the IERW is adapted from the study by Palakkal et al.[19]

conventional ED can be achieved by a chemical process or by hydrodynamic instabilities,[34] surface conduction and electro-osmosis are the two dominant mechanisms that enable overlimiting current in shock ED.[29,32,35] By promoting these pathways for charge transfer, IERWs are more ionically conductive and thus reduce the electrical resistance across the device compared to borosilicate glass.[36,37] In dilute solutions, ion exchange resins generally prefer the ion with the highest charge and lowest degree of hydration,[38] which makes these materials suitable for applications that require multivalent selectivity. As shown in Figure 1, the deionization shock in shock IX splits the contaminated feed into depleted and enriched product streams, which are continuously separated by driving a flow perpendicular to the applied electric field.[14,39,40]

2. MATERIALS AND EXPERIMENTAL METHODS

2.1. Device Design and Fabrication. The two devices used here (one for shock ED and the other for shock IX), shown schematically in Figure 1a, are based on a design previously published by our group.[15,21] The only difference between the two devices is the type of porous material used (Figure 1b). Both devices consist of three inlets (two to transport the electrode streams and the third to deliver contaminated feed) and four outlets (two to transport the electrode streams and two to generate depleted and enriched product streams at the splitter). All fluids are transported through 1/8th-inch Tygon tubing (Saint-Gobain) glued onto portplates made of cast acrylic. These portplates seal liquids

inside the device and support the rubber tubing through which fluid flows. Moreover, four 1/16th-inch Viton rubber gaskets (DuPont) are used to seal the device and simultaneously provide channels for the electrode streams. The electrodes are made of platinum meshes (Sigma-Aldrich) which are connected to the Gamry Reference 3000 potentiostat/galvanostat using titanium wires (Alfa Aesar). The electrodes and wires are secured in place by compressible Viton gaskets. Cation exchange membranes (Nafion N115, Ion Power) with a thickness of approximately 130 μm and an area of 1.0 cm^2 are used as fluidic barriers between the electrode channels and the porous material. The porous materials are glued onto acrylic frames using the Devcon 2 Ton Epoxy (McMaster-Carr). The splitter (placed midway down the outlet for ease of assembly) is made of cast acrylic and is sealed against the top face of the porous material using 0.04-inch GORE expanded polytetrafluoroethylene (PTFE) gasket tape. During assembly, holes in all of the acrylic slabs and rubber gaskets are formed using a laser cutter (Universal Laser Systems) and refined with a drill press (Palmgren ten-inch, five-speed bench model). These layers are then stacked and held together with nuts, bolts, and washers made of 316 stainless steel.

2.2. Porous Materials. The first porous material used in this study is a borosilicate frit (Adams & Chittenden Scientific Glass) with ultrafine pores (nominally ranging from 0.9 to 1.4 μm in size), an internal surface area of 1.75 m^2 g^{-1} based on Brunauer–Emmett–Teller theory, a mass density of 1.02 g m^{-3}, a porosity of 0.31, and an approximate dimension of 0.5 cm $\times$ 1.8 cm $\times$ 0.6 cm ($x \times y \times z$). The other material is an IERW, specifically a conventional polyethylene resin wafer,

synthesized by mixing the polyethylene binder (Microthene MN71120), ion exchange resin, and sodium chloride in a ratio of 2:1:0.5 by mass. The ion exchange resin blend is produced using a cation exchange resin (Purolite PFC 100E, which is sulfonated sodium polystyrene crosslinked with divinylbenzene; capacity is 1.9 Eq L^{-1} and density is 1.27 g cm^{-3}) and anion exchange resin (Purolite PFA400, which is quaternary benzyl trimethylammonium chloride polystyrene crosslinked with divinylbenzene; capacity is 1.3 Eq L^{-1} and density is 1.07 g cm^{-3}) in a ratio of 1:1.3. The mixture is packed into a foil-lined mold and hot pressed to >109 °C with two metric tons of force for one hour. The resin wafer is cooled to room temperature under load and then immersed in deionized (DI) water three times for 20 minutes to dissolve the sodium chloride porosigen. This IERW has a capacity of 0.93 Eq L^{-1}, a porosity of 0.27, and the same dimensions as the borosilicate frit.

2.3. Preparation of Feed and Electrode Solutions.
In previous work by our group, we demonstrated the ability of shock ED with a borosilicate frit to selectively separate multivalent ions in the presence of excess competing sodium,[16,21] and we proposed several possible mechanisms for this selectivity in a theoretical study.[23] To simplify the processing and analysis of samples in this study and to isolate the role of the porous material on selectivity, we use an artificial wastewater solution in which all dissolved cations are present in approximately equal proportions, as shown in Table

Table 1. Summary of Results Obtained from Static Ionic Conductivity Measurements

	conductivity (mS cm^{-1})	
spacer material	DI water	0.5 g L^{-1} NaCl
borosilicate frit	0.42 ± 0.03	8.4 ± 0.2
IERW	0.56 ± 0.06	8.7 ± 0.8
solution only	$(0.81 ± 0.02) \times 10^{-3}$	0.946 ± 0.001

2. This solution is prepared by first formulating stock solutions with 1000 times the target concentrations made from cobalt sulfate heptahydrate ($CoSO_4 \cdot 7H_2O$), copper sulfate pentahydrate ($CuSO_4 \cdot 5H_2O$), zinc sulfate heptahydrate ($ZnSO_4 \cdot 7H_2O$), mercury chloride ($HgCl_2$), cadmium chloride ($CdCl_2$), nickel sulfate heptahydrate ($NiSO_4 \cdot 7H_2O$), manganese sulfate monohydrate ($MnSO_4 \cdot H_2O$), and sodium sulfate decahydrate ($Na_2SO_4 \cdot 10H_2O$). (All reagents were obtained from Sigma-Aldrich.) Appropriate volumes of these solutions are then diluted in DI water. In preparing the artificial wastewater, the contaminated feed and analyte are

identical in composition, whereas the catholyte includes an additional dose of hydrochloric acid with a concentration of 10 mM. This dose of acid is added to prevent precipitation of metal hydroxides that could form as a result of hydrogen evolution in the otherwise basic catholyte.

2.4. Experimental Procedure.
Experiments begin by setting the flow rates of all streams: $n \times 0.21$ mL min^{-1} for the electrode streams and $n \times 0.065$ mL min^{-1} for the contaminated feed, where $n = 1, 3, 6$, or 9. These streams are transported using peristaltic pumps equipped with Tygon Chemical tubing (Saint-Gobain), and the flows are made smooth by incorporating hydraulic accumulators (i.e., glass vials). The accumulators are left to pressurize and the system to equilibrate overnight, after which the Gamry is set to operate in galvanostatic mode with periodic polarity reversal (see Section 1 of the Supporting Information). The measured voltage is allowed to stabilize for at least one hour until it reaches a steady state. Samples are collected directly from the device in graduated cylinders and stored in centrifuge tubes for analysis, which include measurement of volume, conductivity, pH, and composition of cations. Conductivity and pH are measured using the Mettler Toledo analytical instruments (SevenCompact pH/Cond S213), and the composition is determined using inductively coupled plasma mass spectrometry (Agilent 7900 ICP−MS). The plasma in ICP−MS is made from argon gas and is supplemented by helium, and we add an indium internal standard at 100 ppb to all of our samples. Quantitative analysis requires calibration of the measurements, which is achieved by processing a set of reference standards and producing a calibration curve. (All standard solutions were obtained from Sigma-Aldrich.) Samples and standard solutions are diluted in 2 vol % nitric acid, prior to analysis by ICP−MS.

2.5. Static Ionic Conductivity of Porous Materials.
Electrochemical impedance spectroscopy (EIS) measurements are conducted on the Nuvant Systems EZstat Pro operated in galvanostatic mode. A two-point probe method is used with a cell consisting of two platinum foil working electrodes adhered to two adjustable stainless-steel collectors in a PTFE housing. A stainless-steel screw is used to adjust the distance between the electrodes to the thickness of the material. EIS is performed with a perturbation of 1 mA in the frequency range of 100 kHz−1 Hz. The high-frequency resistance from the Nyquist plot is used to calculate the (ionic) conductivity κ as

$$\kappa = \frac{t}{AR} \tag{1}$$

Table 2. Composition of Artificial Wastewater Comprising Seven Divalent Heavy Metal Cations and One Monovalent Cation (This Mixture is Used as Feed, Anolyte, and Catholyte)

| species, j	concentration, $C_0^{(j)}$ (mg L^{-1})	potential health effects from ingestion[42−45]	sources of contaminant[42−45]
cobalt (Co^{2+})	12.97	nausea and vomiting	coal-fired power plants, mining, erosion of natural deposits
copper (Cu^{2+})	11.17	gastrointestinal distress, liver and kidney damage	corrosion of pipes, erosion of natural deposits
zinc (Zn^{2+})	10.95	damage to nervous system, dermatitis	refineries, electroplating, metals manufacturing
mercury [Hg(II)]	9.61	damage to nervous system, toxic to kidneys	batteries, paper industry, erosion of natural deposits
cadmium (Cd^{2+})	9.78	renal dysfunction, lung disease, bone defects	welding, electroplating, pesticides
nickel (Ni^{2+})	11.82	dermatitis, allergic reaction	corrosion of pipes, erosion of natural deposits
manganese (Mn^{2+})	10.62	damage to nervous system, toxic	welding, chemicals manufacturing, erosion of natural deposits
sodium (Na^+)	35.39		
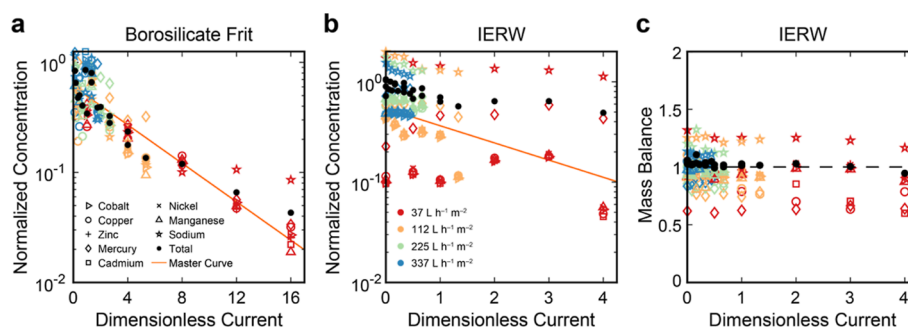
Figure 2. Quantitative analysis of selective ion removal using shock ED and shock IX. Normalized concentration of the cations in the depleted stream (eq 2) versus the dimensionless current (eq 4) using (a) borosilicate frit and (b) IERW. Markers are used to designate different species and colors to designate different productivities (feed flow rate, Q', per unit projected active area). Black circles represent the normalized (total) concentration of all dissolved cations, and the solid lines are guides to the eye. (c) Total mass balance (black circles, eq 3) and mass balances of individual species (colored markers, obtained by omitting the summations in eq 3) versus dimensionless current using the IERW. The total and species mass balances in each of the product streams are shown in Figure S4. A value of one for the mass balance implies no accumulation. Water recovery and energy demand are analyzed in Section 2 of the Supporting Information.

where t is the material thickness, A is the material surface area, and R is the measured resistance. Conductivity is measured in DI water with a 0.5 g L^{-1} solution of NaCl as the supporting electrolyte. The results of these measurements are summarized in Table 1.

3. RESULTS AND DISCUSSION

To compare the performance of the original shock ED method (with borosilicate glass) with that of the new shock IX process, we used an artificial multicomponent mixture comprising seven divalent heavy metal cations and one monovalent cation as the feed. Table 2 shows the composition of this mixture and the potential health effects from ingestion and sources of each contaminant. (We note that the speciation of mercury(II), which includes $Hg(OH)_2$, $HgOH^+$, and Hg^{2+} as prominent species, depends on its concentration and on pH.) In all experiments, we operated the system at constant current because it facilitates the formation of a stable deionization shock wave at overlimiting current.[15] (In contrast, operating at a constant voltage can cause overshoot and oscillation about a desired overlimiting current and is associated with variability in the shock wave[41]). As explained in Section 1, we employed polarity reversal in all experiments in this study to reduce the formation of metal hydroxides and deposits at the electrodes. Our results for selective separation of heavy metals from this multicomponent mixture are presented in Figure 2, where the normalized concentration of species j in the depleted stream is defined as

$$\tilde{C}_D^{(j)} = \frac{C_D^{(j)}}{C_0^{(j)}} \tag{2}$$

total mass balance as

$$\mu = \frac{\sum_j [C_D^{(j)} Q' \gamma + C_E^{(j)} Q' (1 - \gamma) + (C_C^{(j)} + C_A^{(j)})Q]}{\sum_j C_0^{(j)}(Q' + 2Q)}, \gamma$$

$$= \frac{Q_D}{Q'} \tag{3}$$

(γ is water recovery), and dimensionless current as

$$\tilde{I} = \frac{I}{I_{lim}} \tag{4}$$

values of $C_0^{(j)}$ are provided in Table 2; values of $C_D^{(j)}$, $C_E^{(j)}$, $C_C^{(j)}$, and $C_A^{(j)}$ are measured experimentally. In eq 4, I is the applied current, and I_{lim} is the flow-limited current

$$I_{lim} = \sum_j \frac{\nu^{(j)} C_0^{(j)} F Q'}{M^{(j)}} \tag{5}$$

where ν is valence (charge), C is the mass concentration, F is Faraday's constant, Q' is the volumetric flow rate of the feed, M is molar mass, and the sum is taken over all cations as j. This definition of limiting current can be interpreted as the rate of forced convection of positive charge carriers into the device, and it is assumed that the flux of anions is zero at the steady state in the presence of ideal cation exchange membranes.

Figure 2a shows that the concentration of ions in the depleted stream decreases with increasing current when using the borosilicate frit. (Ion removal that occurs when no current is applied is due to exchange of H^+ in the catholyte with cations in the feed channel across the bottom membrane.) This material, however, provides only limited selectivity toward the multivalent ions, relative to sodium (Figure 3a), where selectivity becomes prominent at high current. In this study, (retention) selectivity is defined as

$$S_{j:k} = \frac{C_D^{(k)}/C_D^{(j)}}{C_0^{(k)}/C_0^{(j)}} = \frac{C_D^{(k)}/C_0^{(k)}}{C_D^{(j)}/C_0^{(j)}} = \frac{\tilde{C}_D^{(k)}}{\tilde{C}_D^{(j)}} \tag{6}$$

which may be interpreted as the ratio of the concentration of species k to that of species j in the depleted stream, scaled by the corresponding ratio of feed concentrations (if $S_{j:k} > 1$, then species j is selectively removed, relative to species k). Figure 2b shows that the concentration of ions in the depleted stream decreases with increasing current when using the IERW, though, in contrast to the borosilicate frit, the IERW provides massive selectivity toward the multivalent ions (Figure 3b), where little to no sodium is removed in the process. The total mass balance in Figure 2c indicates that the system was operated at the steady state, with no accumulation of mass in the device ($\mu = 1$). We note, however, that there may be accumulation of individual species (primarily the multivalent ions, $\mu^{(j)} < 1$) due to their exchange with other previously adsorbed species (primarily sodium, $\mu^{(Na)} > 1$).

Multivalent ion selectivity in shock ED was observed in our previous experimental work,[16,17,21] and its mechanisms were
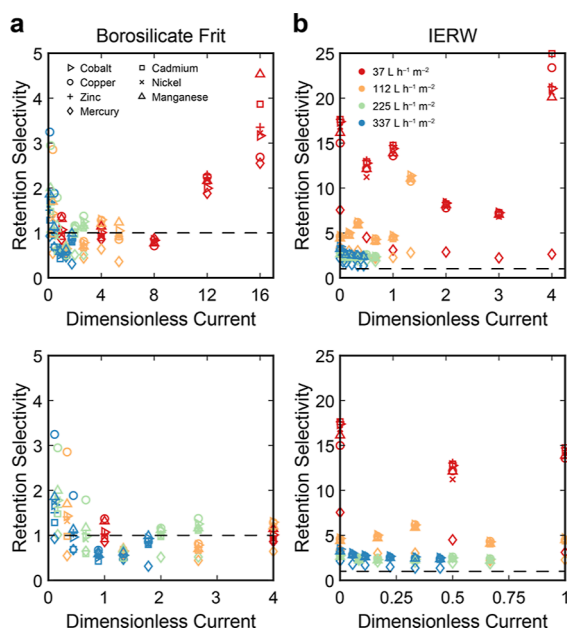
Figure 3. Comparison of multivalent ion selectivity (eq 6, with species k taken as sodium) versus dimensionless current using (a) shock ED and (b) shock IX. The lower two panels represent a magnified view of the upper two. Markers are used to designate different species and colors to designate different productivities.

examined in our subsequent theoretical studies.[22,23] In this paper, we demonstrate for the first time that multivalent ion selectivity in shock ED (or shock IX when using an IERW) can be significantly boosted by using a class of porous materials with known selective properties. Figure 3a shows that retention selectivity is small (near one), except at high currents, when using the borosilicate frit, even though the fraction of ions removed is large (Figure 2a). On the other hand, Figure 3b shows that retention selectivity is large, especially at low flow rates, when using the IERW. A lower flow rate increases the contact time between solution and resin, which likely leads to more favorable ion exchange kinetics (e.g., diffusion of ions toward and within resin beads and adsorption of ions) and greater transport of divalent species by surface conduction in the direction of the applied current. The mechanism underlying the sharp increase in selectivity in Figure 3b is undetermined, but we suspect that selectivity should increase monotonically with the applied current, as shown in the case in Figure 3a. This observation suggests that the values of selectivity at dimensionless currents of 2 and 3 are oddly low, which could be due to disproportionate accumulation of the multivalent cations in the enriched stream, as shown in Figure S4 (top right panel).

The selectivity we obtained using shock IX is large even when compared to specialized capacitive deionization (CDI) systems that use intercalation electrodes, such as Prussian blue analogues. For example, Singh et al. developed a CDI system with two identical nickel hexacyanoferrate (NiHCF) electrodes
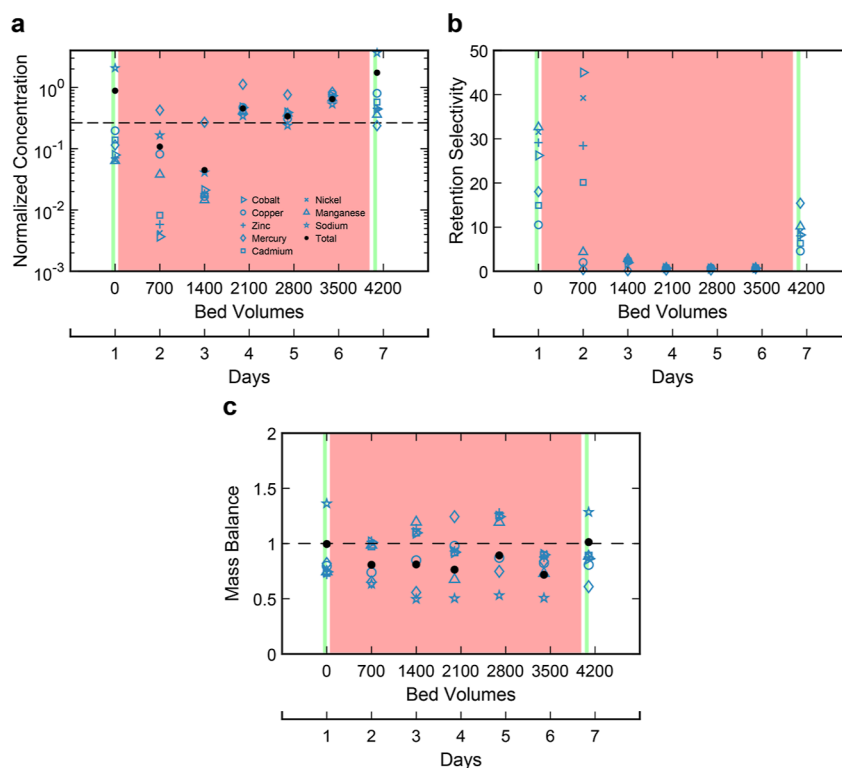

Figure 4. Quantitative analysis of the dynamics and time dependence of ion removal by shock IX. (a) Normalized concentration and (b) retention selectivity (relative to sodium) of the cations in the depleted stream versus time. The dashed line in (a) represents the maximum ion removal achieved by ion exchange alone ($\tilde{I} = 0$; see Figure S3). (c) Total mass balance and mass balances of individual species versus time; balances in each of the product streams are shown in Figure S5. One bed volume equals the total volume of the porous IERW multiplied by its porosity (see Section 2.2). Markers are used to designate different species, and black circles represent the normalized (total) concentration of all dissolved cations. Regions colored green correspond to a feed of 0.1 M NaCl ($\tilde{I} = 0$ and $Q' = 111$ L h^{-1} m^{-2}), and the region colored red corresponds to the feed in Table 2 ($\tilde{I} = 2$ and $Q' = 37$ L h^{-1} m^{-2}).

to selectively separate sodium (monovalent) from magnesium and calcium (divalent).[46] In one experiment, the concentration of sodium was reduced from 20 mM to approximately 12 mM, and the concentrations of magnesium and calcium were reduced from 20 mM to approximately 19.6 mM,[46] which corresponds to a retention selectivity of $S_{Na:Mg} \approx S_{Na:Ca} = 1.6$. In another example, Singh et al. developed a CDI system with two identical vanadium hexacyanoferrate (VHCF) electrodes to selectively remove divalent cations from water.[47] In one experiment, the concentration of sodium was reduced from 10 mM to approximately 7.2 mM, and the concentration of calcium was reduced from 10 mM to approximately 5.1 mM,[47] which corresponds to a retention selectivity of $S_{Ca:Na} = 1.4$. These results are representative of the extent of cation retention selectivity that can be achieved using CDI and intercalation technologies.[48,49] Also, while multivalent selectivity by shock IX is comparatively large, the values shown in Figure 3 can be increased further for instance by using advanced electrodes to drive current by divalent ion intercalation.[47,49,50]

Since ion exchange resins have inherent loading capacities and ion affinity orders, we expect there to be non-steady substitution of adsorbed ions on the IERW, as suggested by Figure 2c. In particular, the overall mass balance shows that more sodium exits the system than is fed, whereas all divalent cations exhibit the opposite trend. It is known in the EDI literature that ion exchange resins are at least partially regenerated by the action of H^+ and OH^- produced via water splitting at bipolar junctions,[51−53] and we expect this to be the case in shock IX as well. To study the dynamics and time dependence of ion separation by shock IX in greater detail, we performed a continuous experiment spanning one week, and the results are shown in Figure 4. We began the experiment by feeding a 0.1 M NaCl solution at 111 L h^{-1} m^{-2} ($\tilde{I} = 0$) for two hours to preload the cation exchange resin with sodium. After that, the multicomponent mixture shown in Table 2 was fed at 37 L h^{-1} m^{-2} for 6 days (with either $\tilde{I} = 0$ or $\tilde{I} = 2$), and samples were collected periodically to quantify performance. When no current was applied, we observed ion exchange with replacement of the preloaded sodium with divalent cations, as shown in Figure 4a. We note that the hydrochloric acid in the catholyte (see Section 2.3) partly contributes to transport of ions out of the feed when no current is applied. To further quantify the extent of ion removal by ion exchange alone, we repeated the experiment shown in Figure 4 but without applying the current, as explained in Section 3 of the Supporting Information. Figure S3a shows that ion removal by ion exchange was in the range of 60−75% for the divalent cations, and breakthrough (or resin exhaustion) was reached at approximately 500 bed volumes.

Figure 4a,b shows that the applied current significantly increased both ion removal and retention selectivity—with over 99% removal of four out of the seven divalent cations—and delayed the onset of breakthrough compared to ion exchange alone. However, both ion removal and selectivity decreased to steady values over time, which suggests that the electroregeneration of resin surfaces by protons produced at the anode may not be sufficient to operate the system continuously over long periods of time. These results imply that stable, long-term operation can be achieved either by optimizing the rate at which protons are produced via electrolysis or by introducing a brief, periodic cleaning step using a benign solution such as 0.1 M NaCl (regions colored green in Figure 4).[54,55] In mixed-ion exchange resin beds and wafers, it is known that hydroxide is generated via water splitting in regions of ion depletion at the interfaces between oppositely charged surfaces (e.g., cation exchange membrane and anion exchange resin).[56,57] The results in Figure 4c show accumulation ($\mu < 1$) of species in the device, which may be explained by the fact that heavy metal cations react with these hydroxide ions to produce insoluble metal hydroxides.[56] This observation is supported by the measured increase in the hydrodynamic resistance (and, in turn, pressure drop) in our device, and it implies that the metal hydroxides form films[58] on the resin beads and physically plug the compartments of the wafer. This phenomenon also occurs in EDI systems when used to remove heavy metal cations from water,[56−58] and one proposed solution is to design a vertically layered bed of cation, anion, and mixed-ion exchange resins to better manage ion removal and prevent precipitation reactions.[56,59] This kind of system requires complex stack design and operation, whereas shock IX can potentially achieve the same device durability by using a homogeneous cation exchange resin wafer with cation exchange membranes. Future work will thus focus on designing homogeneous and layered IERWs to reduce water splitting and prevent precipitation of metal hydroxides in shock IX.

4. ENVIRONMENTAL IMPLICATIONS

Metals and metalloids exist in virtually all ecosystems, and their natural concentrations vary depending on the local geology. Occurrences such as a land disturbance in metal-rich areas can lead to erosion and mobilization of these elements into nearby water streams. Similarly, human and industrial activities may redistribute and concentrate metals in areas that are not naturally enriched in these species, and often there is no visible evidence of water contamination. While some metals are essential as nutrients (e.g., iron), all metals are toxic above a certain level, and in fact, some are toxic even in trace quantities (e.g., lead, mercury, and cadmium). In this study, we demonstrated that systems based on deionization shock waves can efficiently and selectively remove toxic metal cations from dilute feeds. This capability often cannot be economically achieved using membrane technologies which have an energy requirement that scales with the volume of water treated, as opposed to the amount of salt removed.[24] We also showed that the use of shock IX with an IERW is a viable approach to electrify traditional ion exchange and eliminate the need for frequent regeneration using strong acids. The hybrid shock IX method exhibits greater ion removal and selectivity, for longer periods of time, compared to the use of ion exchange alone. Shock IX also displays greater multivalent ion selectivity compared to other electrochemical methods such as EDI (which actually comprises selective ion exchange resins) and CDI with intercalation electrodes. These attractive properties make shock IX a viable method for tackling heavy metal pollution and a suitable technology in general for selective ion separations.

■ ASSOCIATED CONTENT

ⓈI Supporting Information

The Supporting Information is available free of charge at https://pubs.acs.org/doi/10.1021/acs.est.2c05042.

> Analysis of shock ED with polarity reversal, water recovery and energy demand data, analysis of ion

removal with no applied current, and auxiliary mass balance data (PDF)

■ AUTHOR INFORMATION

Corresponding Author

Martin Z. Bazant − *Department of Chemical Engineering and Department of Mathematics, Massachusetts Institute of Technology, Cambridge, Massachusetts 02139, United States;* ● orcid.org/0000-0002-8200-4501; Email: bazant@mit.edu

Authors

Mohammad A. Alkhadra − *Department of Chemical Engineering, Massachusetts Institute of Technology, Cambridge, Massachusetts 02139, United States;* ● orcid.org/0000-0003-3866-709X

Matthew L. Jordan − *Cain Department of Chemical Engineering, Louisiana State University, Baton Rouge, Louisiana 70803, United States*

Huanhuan Tian − *Department of Chemical Engineering, Massachusetts Institute of Technology, Cambridge, Massachusetts 02139, United States;* ● orcid.org/0000-0001-5515-9105

Christopher G. Arges − *Department of Chemical Engineering, Pennsylvania State University, University Park, Pennsylvania 16802, United States*

Complete contact information is available at:
https://pubs.acs.org/10.1021/acs.est.2c05042

Notes

The authors declare no competing financial interest.

■ ACKNOWLEDGMENTS

■ REFERENCES

(1) Fu, F.; Wang, Q. Removal of heavy metal ions from wastewaters: a review. *J. Environ. Manage.* **2011**, *92*, 407−418.

(2) Lakherwal, D. Adsorption of heavy metals: a review. *Int. J. Environ. Res. Dev.* **2014**, *4*, 41−48.

(3) Ahmed, M. J. K.; Ahmaruzzaman, M. A review on potential usage of industrial waste materials for binding heavy metal ions from aqueous solutions. *J. Water Process. Eng.* **2016**, *10*, 39−47.

(4) Carolin, C. F.; Kumar, P. S.; Saravanan, A.; Joshiba, G. J.; Naushad, M. Efficient techniques for the removal of toxic heavy metals from aquatic environment: A review. *J. Environ. Chem. Eng.* **2017**, *5*, 2782−2799.

(5) Vaishya, R. C.; Gupta, S. K. Coated sand filtration: an emerging technology for water treatment. *J. Water Supply: Res. Technol.–AQUA* **2003**, *52*, 299−306.

(6) Esalah, J.; Husein, M. M. Removal of heavy metals from aqueous solutions by precipitation-filtration using novel organo-phosphorus ligands. *Sep. Sci. Technol.* **2008**, *43*, 3461−3475.

(7) Yurekli, Y.; Yildirim, M.; Aydin, L.; Savran, M. Filtration and removal performances of membrane adsorbers. *J. Hazard. Mater.* **2017**, *332*, 33−41.

(8) Ahmed, S.; Chughtai, S.; Keane, M. A. The removal of cadmium and lead from aqueous solution by ion exchange with Na—Y zeolite. *Sep. Purif. Technol.* **1998**, *13*, 57−64.

(9) Chen, J. P.; Wang, L. Characterization of a Ca-alginate based ion-exchange resin and its applications in lead, copper, and zinc removal. *Sep. Sci. Technol.* **2001**, *36*, 3617−3637.

(10) Petrus, R.; Warchoł, J. K. Heavy metal removal by clinoptilolite. An equilibrium study in multi-component systems. *Water Res.* **2005**, *39*, 819−830.

(11) Kurniawan, T. A.; Chan, G. Y.; Lo, W.-H.; Babel, S. Physico-chemical treatment techniques for wastewater laden with heavy metals. *Chem. Eng. J.* **2006**, *118*, 83−98.

(12) Qiu, W.; Zheng, Y. Removal of lead, copper, nickel, cobalt, and zinc from water by a cancrinite-type zeolite synthesized from fly ash. *Chem. Eng. J.* **2009**, *145*, 483−488.

(13) Kemmer, F. N.; McCallion, J. *The NALCO Water Handbook*; McGraw-Hill: New York, 1979; pp 1−750.

(14) Schlumpberger, S.; Lu, N. B.; Suss, M. E.; Bazant, M. Z. Scalable and Continuous Water Deionization by Shock Electrodialysis. *Environ. Sci. Technol. Lett.* **2015**, *2*, 367−372.

(15) Alkhadra, M. A.; Conforti, K. M.; Gao, T.; Tian, H.; Bazant, M. Z. Continuous Separation of Radionuclides from Contaminated Water by Shock Electrodialysis. *Environ. Sci. Technol.* **2019**, *54*, 527−536.

(16) Alkhadra, M. A.; Gao, T.; Conforti, K. M.; Tian, H.; Bazant, M. Z. Small-scale desalination of seawater by shock electrodialysis. *Desalination* **2020**, *476*, 114219.

(17) Conforti, K. M.; Bazant, M. Z. Continuous ion-selective separations by shock electrodialysis. *AIChE J.* **2020**, *66*, No. e16751.

(18) Pan, S.-Y.; Snyder, S. W.; Ma, H.-W.; Lin, Y. J.; Chiang, P.-C. Development of a resin wafer electrodeionization process for impaired water desalination with high energy efficiency and productivity. *ACS Sustainable Chem. Eng.* **2017**, *5*, 2942−2948.

(19) Palakkal, V. M.; Valentino, L.; Lei, Q.; Kole, S.; Lin, Y. J.; Arges, C. G. Advancing electrodeionization with conductive ionomer binders that immobilize ion-exchange resin particles into porous wafer substrates. *npj Clean Water* **2020**, *3*, 5.

(20) Jordan, M. L.; Valentino, L.; Nazyrynbekova, N.; Palakkal, V. M.; Kole, S.; Bhattacharya, D.; Lin, Y. J.; Arges, C. G. Promoting water-splitting in Janus bipolar ion-exchange resin wafers for electrodeionization. *Mol. Syst. Des. Eng.* **2020**, *5*, 922−935.

(21) Tian, H.; Alkhadra, M. A.; Conforti, K. M.; Bazant, M. Z. Continuous and Selective Removal of Lead from Drinking Water by Shock Electrodialysis. *ACS ES&T Water* **2021**, *1*, 2269−2274.

(22) Tian, H.; Alkhadra, M. A.; Bazant, M. Z. Theory of shock electrodialysis I: Water dissociation and electrosmotic vortices. *J. Colloid Interface Sci.* **2021**, *589*, 605−615.

(23) Tian, H.; Alkhadra, M. A.; Bazant, M. Z. Theory of shock electrodialysis II: Mechanisms of selective ion removal. *J. Colloid Interface Sci.* **2021**, *589*, 616−621.

(24) Alkhadra, M. A. e. a.; Su, X.; Suss, M. E.; Tian, H.; Guyes, E. N.; Shocron, A. N.; Conforti, K. M.; de Souza, J. P.; Kim, N.; Tedesco, M.; Khoiruddin, K.; Wenten, I. G.; Santiago, J. G.; Hatton, T. A.; Bazant, M. Z. Electrochemical Methods for Water Purification, Ion Separations, and Energy Conversion. *Chem. Rev.* **2022**, *122*, 13547−13635.

(25) Zhang, Z.; Chen, A. Simultaneous removal of nitrate and hardness ions from groundwater using electrodeionization. *Sep. Purif. Technol.* **2016**, *164*, 107−113.

(26) Rodgers, B. Electrodeionization versus Electrodialysis: A Clean-Up of Produced Water in Hydraulic Fracturing. Ph.D. Thesis, University of Arkansas, 2016.

(27) Ulusoy Erol, H. B.; Hestekin, C. N.; Hestekin, J. A. Effects of resin chemistries on the selective removal of industrially relevant metal ions using wafer-enhanced electrodeionization. *Membranes* **2021**, *11*, 45.

(28) Mani, A.; Bazant, M. Z. Deionization shocks in microstructures. *Phys. Rev. E* **2011**, *84*, 061504.

(29) Deng, D.; Dydek, E. V.; Han, J.-H.; Schlumpberger, S.; Mani, A.; Zaltzman, B.; Bazant, M. Z. Overlimiting current and shock electrodialysis in porous media. *Langmuir* **2013**, *29*, 16167−16177.

(30) Han, J.-H.; Khoo, E.; Bai, P.; Bazant, M. Z. Over-limiting current and control of dendritic growth by surface conduction in nanopores. *Sci. Rep.* **2014**, *4*, 7056.

(31) Han, J.-H.; Wang, M.; Bai, P.; Brushett, F. R.; Bazant, M. Z. Dendrite suppression by shock electrodeposition in charged porous media. *Sci. Rep.* **2016**, *6*, 28054.

(32) Dydek, E. V.; Zaltzman, B.; Rubinstein, I.; Deng, D.; Mani, A.; Bazant, M. Z. Overlimiting current in a microchannel. *Phys. Rev. Lett.* **2011**, *107*, 118301.

(33) Alizadeh, S.; Bazant, M. Z.; Mani, A. Impact of network heterogeneity on electrokinetic transport in porous media. *J. Colloid Interface Sci.* **2019**, *553*, 451−464.

(34) Nikonenko, V. V.; Kovalenko, A. V.; Urtenov, M. K.; Pismenskaya, N. D.; Han, J.; Sistat, P.; Pourcelly, G. Desalination at overlimiting currents: State-of-the-art and perspectives. *Desalination* **2014**, *342*, 85−106.

(35) Nam, S.; Cho, I.; Heo, J.; Lim, G.; Bazant, M. Z.; Moon, D. J.; Sung, G. Y.; Kim, S. J. Experimental verification of overlimiting current by surface conduction and electro-osmotic flow in micro-channels. *Phys. Rev. Lett.* **2015**, *114*, 114501.

(36) Lee, J.-W.; Yeon, K.-H.; Song, J.-H.; Moon, S.-H. Character-ization of electroregeneration and determination of optimal current density in continuous electrodeionization. *Desalination* **2007**, *207*, 276−285.

(37) Wenten, I.; Khoiruddin, K.; Alkhadra, M. A.; Tian, H.; Bazant, M. Z. Novel ionic separation mechanisms in electrically driven membrane processes. *Adv. Colloid Interface Sci.* **2020**, *284*, 102269.

(38) Clifford, D. A. *Water Quality and Treatment: A Handbook of Community Water Supplies*, 5th edn.; McGraw-Hill, Inc., 1999; pp 9.1−9.91.

(39) Dydek, E. V.; Bazant, M. Z. Nonlinear dynamics of ion concentration polarization in porous media: The leaky membrane model. *AIChE J.* **2013**, *59*, 3539−3555.

(40) Bazant, M. Z.; Dydek, E. V.; Deng, D.; Mani, A. Method and apparatus for desalination and purification. U.S. Patent 8,801,910 B2, 2014.

(41) Zangle, T. A.; Mani, A.; Santiago, J. G. On the Propagation of Concentration Polarization from Microchannel−Nanochannel Inter-faces Part II: Numerical and Experimental Study. *Langmuir* **2009**, *25*, 3909−3916.

(42) Sharma, S. K. *Heavy Metals in Water: Presence, Removal and Safety*; Royal Society of Chemistry, 2014; pp 1−24.

(43) Anton, M.-C.; Rojas, M. B.; Aluculesei, A.; Marguba, R.; Dorohoi, D. Study regarding the water pollution in Romania and Spain. *Rom. J. Phys.* **2008**, *53*, 157−163.

(44) Singh, R.; Gautam, N.; Mishra, A.; Gupta, R. Heavy metals and living systems: An overview. *Indian J. Pharmacol.* **2011**, *43*, 246.

(45) Fahimirad, S.; Hatami, M. *Medicinal Plants and Environmental Challenges*; Springer, 2017; pp 189−214.

(46) Singh, K.; Qian, Z.; Biesheuvel, P.; Zuilhof, H.; Porada, S.; de Smet, L. C. Nickel hexacyanoferrate electrodes for high mono/divalent ion-selectivity in capacitive deionization. *Desalination* **2020**, *481*, 114346.

(47) Singh, K.; Li, G.; Lee, J.; Zuilhof, H.; Mehdi, B. L.; Zornitta, R. L.; Smet, L. C. Divalent Ion Selectivity in Capacitive Deionization with Vanadium Hexacyanoferrate: Experiments and Quantum-Chemical Computations. *Adv. Funct. Mater.* **2021**, *31*, 2105203.

(48) Gamaethiralalage, J.; Singh, K.; Sahin, S.; Yoon, J.; Elimelech, M.; Suss, M.; Liang, P.; Biesheuvel, P.; Zornitta, R. L.; de Smet, L. Recent advances in ion selectivity with capacitive deionization. *Energy Environ. Sci.* **2021**, *14*, 1095−1120.

(49) Uwayid, R.; Guyes, E. N.; Shocron, A. N.; Gilron, J.; Elimelech, M.; Suss, M. E. Perfect divalent cation selectivity with capacitive deionization. *Water Res.* **2022**, *210*, 117959.

(50) Srimuk, P.; Lee, J.; Fleischmann, S.; Aslan, M.; Kim, C.; Presser, V. Potential-Dependent, Switchable Ion Selectivity in Aqueous Media Using Titanium Disulfide. *ChemSusChem* **2018**, *11*, 2091−2100.

(51) Meng, H.; Peng, C.; Song, S.; Deng, D. Electro-regeneration mechanism of ion-exchange resins in electrodeionization. *Surf. Rev. Lett.* **2004**, *11*, 599−605.

(52) Song, J.-H.; Yeon, K.-H.; Moon, S.-H. Transport Characteristics of Co^{2+} Through an Ion Exchange Textile in a Continuous Electrodeionization (CEDI) System Under Electro-Regeneration. *Sep. Sci. Technol.* **2005**, *39*, 3601−3619.

(53) Lu, J.; Wang, Y.-X.; Lu, Y.-Y.; Wang, G.-L.; Kong, L.; Zhu, J. Numerical simulation of the electrodeionization (EDI) process for producing ultrapure water. *Electrochim. Acta* **2010**, *55*, 7188−7198.

(54) Fedorenko, V. Ultrapure water production using continuous electrodeionization. *Pharm. Chem. J.* **2003**, *37*, 157−160.

(55) Feng, X.; Wu, Z.; Chen, X. Removal of metal ions from electroplating effluent by EDI process and recycle of purified water. *Sep. Purif. Technol.* **2007**, *57*, 257−263.

(56) Yeon, K.-H.; Song, J.-H.; Moon, S.-H. A study on stack configuration of continuous electrodeionization for removal of heavy metal ions from the primary coolant of a nuclear power plant. *Water Res.* **2004**, *38*, 1911−1921.

(57) Lu, H.; Wang, Y.; Wang, J. Removal and recovery of Ni^{2+} from electroplating rinse water using electrodeionization reversal. *Desalination* **2014**, *348*, 74−81.

(58) Jiang, B.; Li, F.; Zhao, X. Removal of trace Cs(I), Sr(II), and Co(II) in aqueous solutions using continuous electrodeionization (CEDI). *Desalin. Water Treat.* **2019**, *155*, 175−182.

(59) Yeon, K.-H.; Moon, S.-H. A study on removal of cobalt from a primary coolant by continuous electrodeionization with various conducting spacers. *Sep. Sci. Technol.* **2003**, *38*, 2347−2371.